Oxidation of alkyl benzenes by a flavin photooxidation catalyst on nanostructured metal-oxide films

Prateek Dongare[a], Ian MacKenzie[a], Degao Wang[a], David A. Nicewicz[a,1], and Thomas J. Meyer[a,1]

[a]Department of Chemistry, University of North Carolina at Chapel Hill, Chapel Hill, NC 27599

Contributed by Thomas J. Meyer, June 22, 2017 (sent for review May 3, 2017; reviewed by James M. Mayer and David G. Whitten)

We describe here a surface-bound, oxide-based procedure for the photooxidation of a family of aromatic hydrocarbons by a phosphate-bearing flavin mononucleotide (FMN) photocatalyst on high surface area metal-oxide films.

flavin | excited state | photooxidation | oxide surface | alkyl benzene

An important element in synthetic organic chemistry has been the development and application of organic excited states in solution, either by sensitization or electron transfer catalysis (1). Exploitation of organic excited states has evolved from the bench scale to the photochemical reactor scale. In a parallel effort, with a different focus, advances have also been made in exploiting nanoparticle oxide surfaces for energy conversion applications based on chemically bound molecular reactants (2). An advantage of the latter is maximization of the local microscopic surface volume for enhancing efficiencies. We describe here the integration of the two areas with the goal of creating stable photochemical environments that minimize reaction volumes in photooxidation reactions.

Our experiments exploit the excited states of the flavin cofactors found in riboflavin (vitamin B_2), flavin mononucleotide (FMN), and flavin adenine dinucleotide. They are potent photocatalysts and play important roles in biological reactions (3–6). In its redox properties, FMN is more flexible than nicotinamide adenine dinucleotide (NAD) as a donor because it can participate in either $1e^-$ or $2e^-$ transfer reactions (Eq. **1**) as opposed to NAD, which undergoes $2e^-$ hydride transfer (7–9).

$$\mathrm{FMN}_{(ox)} \underset{-e^-,\,-H^+}{\overset{e^-,\,H^+}{\rightleftharpoons}} \mathrm{FMNH}^{\bullet} \underset{-e^-,\,-H^+}{\overset{e^-,\,H^+}{\rightleftharpoons}} \mathrm{FMNH}_{2(red)} \qquad (1)$$

Analogous to quinones, FMN can exist in three redox states—oxidized (flavin-quinone), one-electron reduced (flavin-semiquinone), and two-electron reduced (flavin-hydroquinone) (8). Riboflavin-based organocatalysis has been explored as a green and economic alternative to metal catalyzed reactions (10) in the photooxidation of alkyl benzenes, amino acids, phenols, saccharides, water, and other substrates (4, 11–17).

In the current study, we have explored an FMN photocatalyst bound to nanoparticle transparent metal-oxide surfaces in the C–H oxygenation of alkyl benzenes. The FMN derivative consists of the iso-alloxazine, ribityl, and phosphate groups as shown in Fig. 1. In the absence of external electron transfer donors, the ribityl group undergoes intramolecular photooxidation, reducing the iso-alloxazine and rendering the riboflavin photosensitive. In the current application, the phosphate group also serves to bind the FMN dye to oxide surfaces.

The photophysics and photooxidation of the flavins have been investigated earlier (18). Upon irradiation with blue light, the FMN chromophore forms a lowest-energy singlet-excited state (^{1}FMN) with high efficiency. It is a potent oxidant with an excited-state reduction potential ($FMN^*/FMN^{-\bullet}$) of +1.77 V vs. saturated calomel electrode with the ability of oxidizing substrates with potentials <1.8 V (19). In the photooxidation of alkyl benzenes, Megerle et al. have reported that electron transfer (ET) occurs from the triplet state, ^{3}FMN (20, 21), accessed after rapid intersystem crossing (7.8 ns in water) (15, 18). ET to ^{3}FMN, or proton-coupled electron transfer (PCET) (22), oxidizes the alkyl aromatic substrate within 6 μs in 1:1 vol/vol H_2O/MeCN to give a dihydroflavin intermediate ($FMNH_2$) (23). $FMNH_2$ is subsequently reoxidized to the ground state with oxygen as the terminal oxidant (17, 24, 25). A mechanism analogous to methoxybenzyl alcohol oxidation by riboflavin tetraacetate in 1:1 vol/vol H_2O/MeCN by Megerle et al. (18) is shown in Eqs. **2**–**4**. In an alternate pathway, formation of an alkyl benzene radical in the presence of oxygen has the capability to initiate radical chains, as the peroxyl radicals are very reactive with their corresponding alkyl benzene form. As pointed out earlier, there is a possibility of contributions in overall catalysis from competitive pathways (26). However, the mechanistic details for the reactions cited here remain to be established in detail, but there is evidence for the involvement of multiple pathways including a possible role for PCET (22, 27). A putative mechanism is shown in Scheme 1.

$$\mathrm{FMN} \xrightarrow[440\ \mathrm{nm}]{h\nu} {}^1\mathrm{FMN}^* \xrightarrow{\mathrm{ISC}} {}^3\mathrm{FMN}^* \qquad (2)$$

$$^3\mathrm{FMN}^* + \text{  } \xrightarrow{2e^-/2H^+} \mathrm{FMNH_2} + \text{ 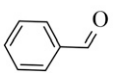 } \qquad (3)$$

$$\mathrm{FMNH_2} \xrightarrow{O_2} \mathrm{FMN} + \mathrm{H_2O_2} \qquad (4)$$

The reactivity of flavins, incorporating oxygen as both a reactant and terminal oxidant, makes them good catalysts in aerobic environments. Paradoxically, the use of O_2 as an oxidant in these reactions poses a problem because H_2O_2 is an intermediate (17, 28) and is known to cause degradation of the flavin cofactor resulting in low reaction yields and poor selectivities (15).

To circumvent H_2O_2 as an intermediate, a number of strategies have been explored including the use of transition-metal disproportionation cocatalysts (15, 29), surfactants (30), modification of the flavin (7), and others (11, 31, 32). Mühldorf and Wolf (15) recently added a nonheme iron complex, $[Fe(TPA)(MeCN)_2](ClO_4)_2$ (TPA = Tris(2-pyridylmethyl)amine) as the cocatalyst (29) for the disproportionation of H_2O_2 ($2H_2O_2 \rightarrow O_2 + 2H_2O$) with

Significance

There are significant advantages in organic, interfacial photooxidation catalysis. Surface-bound catalysts on oxide interfaces offer highly reactive assemblies that minimize both catalyst and solution volume. We demonstrate here the oxygenation of alkyl benzenes by a flavin mononucleotide on nanoporous ZrO_2 or TiO_2 surfaces.

Author contributions: P.D. and T.J.M. designed research; P.D., I.M., and D.W. performed research; P.D., I.M., D.A.N., and T.J.M. analyzed data; and P.D., I.M., D.A.N., and T.J.M. wrote the paper.

Reviewers: J.M.M., Yale University; and D.G.W., University of New Mexico.

The authors declare no conflict of interest.

[1]To whom correspondence may be addressed. Email: nicewicz@unc.edu or tjmeyer@unc.edu.

This article contains supporting information online at www.pnas.org/lookup/suppl/doi:10.1073/pnas.1707318114/-/DCSupplemental.

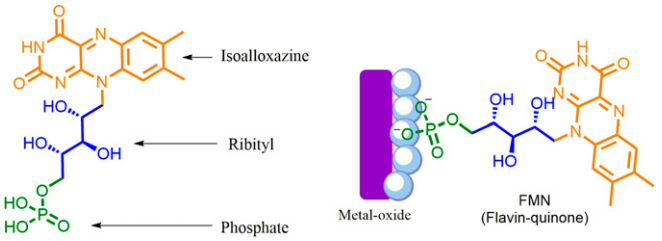

Fig. 1. Structure of flavin mononucleotide (*Left*) and the surface-bound FMN assembly (*Right*) on the surface of ZrO_2 or TiO_2.

notable increases in efficiencies for the photooxidation of alkyl benzenes to ketones and carboxylic acids. Experimental evidence suggested that the increased activity could be attributed to efficient disproportionation of H_2O_2 with a contribution from higher oxidation states of Fe(TPA) in the C–H photooxygenation of the alkyl benzenes.

Extension of the flavin photochemistry to inert surfaces remains largely unexplored. There are examples of flavins immobilized on silica (4) and attached to a polystyrene copolymer (33). However, systematic exploitation of surface binding and flow-through reactors could provide significant synthetic advantages (34). Surface binding to inert, mesoporous oxides minimizes catalyst loading and reaction volumes and subsequently simplifies the reaction conditions and product workup. With transparent metal-oxide supports, a variety of surface-coated reactor designs are available which would be difficult or impossible to achieve with more conventional supports based on silica or polymer beads. In homogeneous catalysis, solubility can also play a major role in the efficiency of a reaction. The majority of the results in the literature on flavin-mediated photooxidations use riboflavin tetraacetate rather than FMN as the photocatalyst because of a gain in catalyst solubility. In heterogeneous catalysis, solubility is no longer a primary factor, allowing the surface-bound FMN to be used with good efficiency.

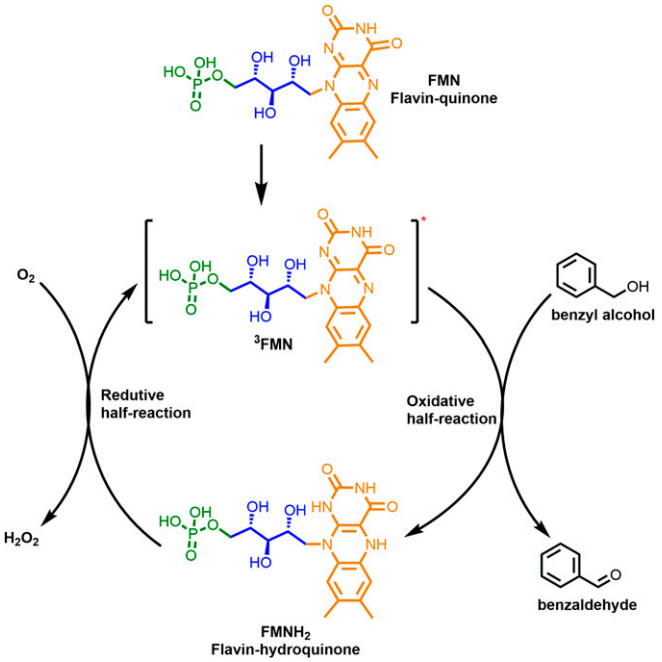

Scheme 1. Generalized mechanism for the photooxidation of benzyl alcohol as a representative substrate by an FTO|ZrO_2-FMN surface in the presence of O_2.

We report here data on surface binding, stabilization, and reactivity of a phosphate-bearing FMN on high surface area, nanoparticle metal-oxide surfaces. As an example, research in this area has resulted in oxide surfaces that have found applications in photoelectrochemical water splitting (2). Techniques are available for preparing optically transparent, nanoparticle surfaces with dimensions in the tens of micrometers with absorptivities sufficient to drive photochemical reactions with high efficiencies even with intense light sources (2). In the experiments described here, 4-μm films of 10-nm nanoparticles of ZrO_2 or 15–20 nm of TiO_2 nanoparticles on fluorine-doped tin oxide (FTO) were added to coated glass substrates (1.0 cm^2). Subsequent addition of the dye to the surface gave films of FTO|ZrO_2|-FMN or FTO|TiO_2|-FMN.

A series of experiments were undertaken to explore the surface properties of the bound dye (see Table 1 and *SI Methods*). Catalyst loading used techniques developed for related photoelectrodes (2). Oxide slides were loaded in 0.5 mM methanol solutions of FMN for up to ∼6 h to achieve the highest surface loadings. The highest surface coverages under these conditions were $\Gamma = 5.7 \times 10^{-11}$ mol cm^{-2} (35). By way of comparison, loading of the metal-to-ligand charge-transfer chromophores $[M(bpy)_2((4,4'\text{-}PO_3H_2)_2bpy)]^{2+}$ (M = Ru, Os, bpy = 2,2′-bipyridine, and 4,4′-$(PO_3H_2)_2$ bpy = 4,4′-bis-(phosphonic acid)-2,2′-bipyridine) under the same conditions result in coverages of $\sim 10^{-10}$ mol/cm^2. Fig. S1 shows the absorption spectrum of a fully loaded FTO|ZrO_2|FMN film with a loading of $\Gamma = 5.7 \times 10^{-11}$ mol cm^{-2} in 1:1 vol/vol MeCN/H_2O.

In the 4-μm films of the oxides used here, the absorption spectrum of the adsorbed dye at its λ_{max} of 450 nm is 0.9. For these high surface area oxide films, the ratio of internal to geometric surface area was ∼1,000 (32). The highest catalyst loading was calculated to be $\sim 5.7 \times 10^{-8}$ mol (<0.1 mol%).

Following surface binding, a major challenge in photocatalytic applications was the stability of the oxide-bound catalyst (36). Upon irradiation with visible light (3-W blue LED, 440 nm) in 1:1 vol/vol MeCN/H_2O, the FMN catalyst desorbed from the surface (Fig. 2, red trace) (37), leading to diminished reactivities. To address issues of surface stability, we performed a series of photostability measurements on modified ZrO_2 and TiO_2 metal-oxide surfaces by time-dependent spectral monitoring of the FMN catalyst at 450 nm (Fig. S2).

Stabilities were assessed by varying solvent polarity in both nitrogen and oxygen atmospheres under LED irradiation. Under most conditions, the catalyst showed full desorption in ∼30 min (Fig. S2). To address the surface stability issue, we attempted to stabilize surface binding on FTO|ZrO_2|-FMN or FTO|TiO_2|-FMN by using a thin coating of a poly(methyl methacrylate) (PMMA) overlayer as described elsewhere for a Ru(II) polypyridyl dye (38). Addition of PMMA did result in greatly increased FMN stability on the oxide surface. Unfortunately, the PMMA layer was unstable in organic solvents and its application was limited to water.

Table 1. List of control experiments with benzylalcohol to benzaldehyde as the model reaction

Entry	Condition	*t*, h	Yield, %
1	FTO|ZrO_2-FMN/ O_2/MnO_2/blue LED	2.5	64
2	FMN/O_2/MnO_2/blue LED	2.5	31
3	No ZrO_2-FMN	2.5	1
4	No O_2	2.5	3
5	Dark	2.5	0
6	Bare ZrO_2	2.5	4
7	No cocatalyst (MnO_2)	2.5	16

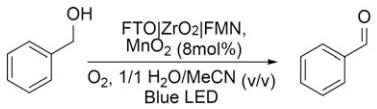

(5)

To stabilize FMN on the surface, we used atomic layer deposition (ALD) to coat the derivatized surfaces with a thin 1.0-nm overlayer of Al_2O_3. The ALD procedure resulted in significant enhancements in stability, for periods of up to ∼3 h (Fig. 2, black). ALD has been used extensively for stabilizing chromophores and chromophore–catalyst assemblies on the surfaces of dye-sensitized photoelectrosynthesis cells for water splitting (2, 39).

With the ALD stabilization of FMN established, a platform was available for exploring C–H photooxidation of alkyl benzenes on the oxide films. Selecting the conversion of benzyl alcohol to benzaldehyde as a model reaction (Eq. **5**), we explored a variety of conditions with results shown in Table 1; in a series of control experiments, we explored the impact of reaction conditions

Table 2. Substrates for photooxidation by FTO|ZrO_2|-FMN with the added MnO_2 cocatalyst, their corresponding products, reaction times, and product yields in 1/1 H_2O:MeCN (vol/vol)

Entry	Substrate(*)	Product	R	t (h)	Yield(†) (%)
1	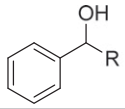	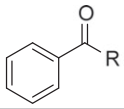	H Me	2.5 2.5	64 59
2	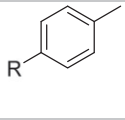	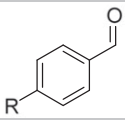	Me tBu	3.0 3.0	72 74
3	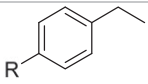	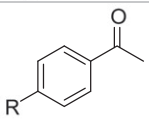	OMe H	2.5 1.0	74 67(‡)
4	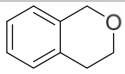	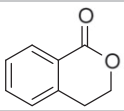	-	2.5	50
5	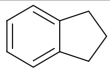	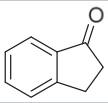	-	2.5	64
6	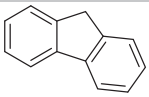	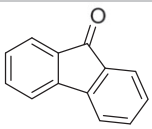	-	2.0	61
7	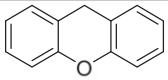	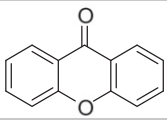	-	2.0	92
8	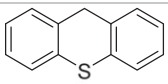	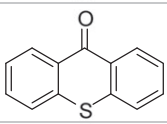	-	0.2	94
9	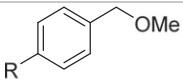	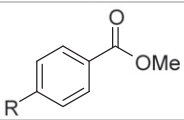	OMe	3.0	71
10		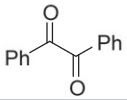	-	2.5	37
11	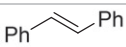	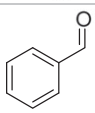	-	2.0	69

*Standard conditions: 0.06 mmol substrate, 8 mol % MnO_2, 1.5 mL 1:1 H_2O:MeCN vol/vol, O_2 saturated, LED (3 W, 450 nm).

†Yields were determined using NMR with hexamethyldisiloxane (HMDSO) as an internal standard.

‡Obtained with added 30 mol % $HClO_4$.

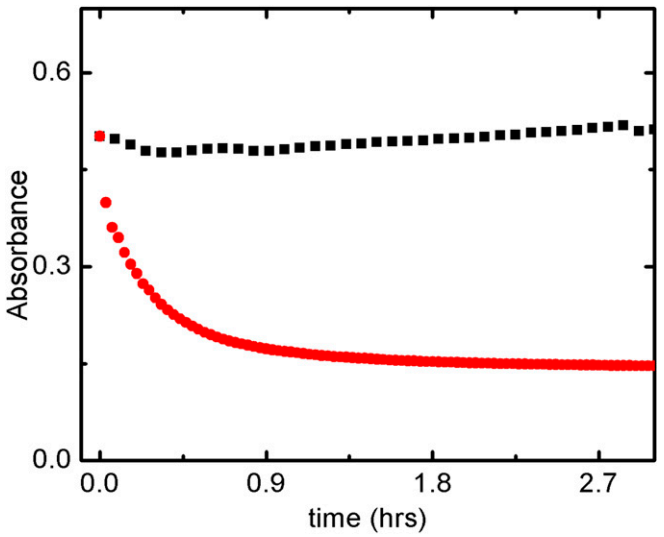

Fig. 2. Spectral changes with time at 450 nm following irradiation of 1.0-cm^2 films loaded with 4-μm-thick FTO|ZrO_2|-FMN films either stabilized with ALD with a 1.0-nm overlayer of Al_2O_3 (black) or unstabilized (red). The data were obtained in 1:1 MeCN/H_2O (vol/vol).

in 1:1 H_2O:MeCN. Variations with light intensity, O_2, and an added cocatalyst were all explored, which ruled out adventitious photooxidation. Based on these experiments, in the absence of FTO|ZrO_2|-FMN, a ZrO_2 surface was unreactive. In homogeneous solutions with added FMN, conversions were lower by a factor of ∼2 compared with the heterogeneous reactions in part due to the limited solubility of the dye, an additional advantage of the surface-bound reactant. (37)

The reactivity of the adsorbed dye on FTO|ZrO_2|-FMN was explored for the substrates shown in Table 2 using the blue LED with 0.06 mmol of substrate and 8 mol % of added MnO_2 or $[Fe(TPA)(MeCN)_2](ClO_4)_2$ (Table S1), in 1:1 H_2O:MeCN (vol/vol). Further experimental details are provided in *SI Methods*.

Benzyl alcohol and 1-phenylethanol were converted to the respective aldehyde and ketone in good yields (Table 2, entry 1). The substituted toluene and ethylbenzene derivatives gave the corresponding aldehydes and acetophenones in good yield (entries 2 and 3). Isochroman, indane, and fluorene (entries 4–6) were all converted into their ketones in moderate to good yields. Xanthene and thioxanthene generated xanthone and thioxanthone in excellent yields (entries 7 and 8) and, for thioxanthene, very short reaction times. Substrate 4-methoxybenzyl methyl ether yielded the benzyl ester in high yield (entry 9). The conversion of tolane to benzil occurs (entry 10), but in reduced yield similar to the corresponding homogeneous reaction (13). Additionally, trans-stilbene (entry 11) underwent photooxygenation to yield benzaldehyde in good yield. A representative set of NMR data is presented in Figs. S3–S5.

We also investigated FTO|TiO_2|-FMN surfaces to explore the role of the oxide surface on reactivity. In the comparative experiments, the product yield was largely the same between oxides. Although no attempt was made in the reaction sequence to exploit the known redox reactivity of TiO_2, given its accessible conduction band (CB) at E_{CB} ∼0 V vs. normal hydrogen electrode, there was no evidence for its involvement in surface reactivity of the dye (37). The latter could be an issue with other reactions, but is of less importance for films of FTO|ZrO_2|-FMN given its 0.5-V-higher CB potential for ZrO_2.

We examined the effect of the deuterated version of the solvent on product yield to rule out participation by singlet oxygen (40). Given its known reactivity, $^1O_2^*$, formed by energy transfer to $^3O_2, ^3FMN^* + {}^3O_2 \rightarrow {}^1O_2^* + FMN$, could play a significant role under our conditions (41). Since the lifetime of singlet oxygen is extended in the deuterated version of the solvent (42), we investigated the oxidation of ethylbenzene, FTO|ZrO_2|-FMN, with added MnO_2 for 1 h in 1/1 D_2O/CD_3CN (vol/vol). Analysis of the products gave a conversion yield of ∼56%, compared with 67% for the nondeuterated solvent 67% (Table 2). In a second experiment, the known singlet oxygen sensitizer, Rose Bengal, was used (10 mol %, 0.01 mmol, 9.7 mg) with benzyl alcohol used (0.1 mmol, 10.4 μL) in 7.5 mL of 1:1 vol/vol H_2O/MeCN. Oxygen was continuously bubbled through the solution while irradiating with green light (520-nm LEDs) for 2.5 h. There was no evidence for the hydrocarbon oxidation product under these conditions.

Conclusions

We have demonstrated here a procedure for a minimum-volume, high-efficiency, organic photochemical reactor. It is based on a surface-bound, flavin-based chromophore on high surface area oxide films. This configuration provides a basis for stable photoredox catalysis in an ultrathin, high surface area nanoparticle reactor.

In the example investigated here, a phosphate-bearing flavin mononucleotide dye was bound to high surface area ZrO_2 or TiO_2 films with surface stabilization by ALD. The modified metal-oxide films demonstrated excellent catalytic activity following irradiation with a 440-nm blue LED. The experiments demonstrate the viability of the approach, one that could be of general value in organic photochemical reactions under conditions that minimize reaction volumes and the time for reaction workup.

For the FMN reactions, the reactivity of the dye on the high surface area oxide films was maintained with high yields obtained for a series of hydrocarbon oxidations. The results presented here provide a basis for extension to larger scales and to catalyst–oxide assemblies with potential applications for larger-scale organic reactions.

Methods

Detailed spectral data and analysis are included in *SI Methods*.

ACKNOWLEDGMENTS. We thank Prof. Chris Dares for help with the reaction setup and preliminary data collection. This research was supported by National Science Foundation Grant CHE-1362481.

1. Romero NA, Nicewicz DA (2016) Organic photoredox catalysis. *Chem Rev* 116: 10075–10166.
2. Ashford DL, et al. (2015) Molecular chromophore–catalyst assemblies for solar fuel applications. *Chem Rev* 115:13006–13049.
3. Metternich JB, Gilmour R (2015) A bio-inspired, catalytic E → Z isomerization of activated olefins. *J Am Chem Soc* 137:11254–11257.
4. Schmaderer H, Hilgers P, Lechner R, König B (2009) Photooxidation of benzyl alcohols with immobilized flavins. *Adv Synth Catal* 351:163–174.
5. Vernon LP (1959) Photochemical oxidation and reduction reactions catalyzed by flavin nucleotides. *Biochim Biophys Acta* 36:177–185.
6. Weber S, Schleicher E (2014) *Flavins and Flavoproteins* (Springer, New York), pp 6–11.
7. König B, et al. (1999) Photoinduced electron transfer in a phenothiazine–riboflavin dyad assembled by zinc–imide coordination in water. *J Am Chem Soc* 121:1681–1687.
8. Tan SL, Webster RD (2012) Electrochemically induced chemically reversible proton-coupled electron transfer reactions of riboflavin (vitamin B2). *J Am Chem Soc* 134: 5954–5964.
9. Tan SLJ, Novianti ML, Webster RD (2015) Effects of low to intermediate water concentrations on proton-coupled electron transfer (PCET) reactions of flavins in aprotic solvents and a comparison with the PCET reactions of quinones. *J Phys Chem B* 119: 14053–14064.
10. Edwards AM (2006) General properties of flavins. *Flavins: Photochemistry and Photobiology* (The Royal Society of Chemistry, Cambridge, UK), Vol 6, pp 1–11.
11. Svoboda J, Schmaderer H, König B (2008) Thiourea-enhanced flavin photooxidation of benzyl alcohol. *Chemistry* 14:1854–1865.
12. Hemmerich P, Massey V, Weber G (1967) Photo-induced benzyl substitution of flavins by phenylacetate: A possible model for flavoprotein catalysis. *Nature* 213: 728–730.
13. Wo J, et al. (2016) Transformation of streptonigrin to streptonigrone: Flavin reductase-mediated flavin-catalyzed concomitant oxidative decarboxylation of picolinic acid derivatives. *ACS Catal* 6:2831–2835.
14. Mühldorf B, Wolf R (2015) Photocatalytic benzylic C-H bond oxidation with a flavin scandium complex. *Chem Commun (Camb)* 51:8425–8428.

15. Mühldorf B, Wolf R (2016) C-H photooxygenation of alkyl benzenes catalyzed by riboflavin tetraacetate and a non-heme iron catalyst. *Angew Chem Int Ed Engl* 55: 427–430.
16. Metternich JB, Gilmour R (2016) One photocatalyst, n activation modes strategy for cascade catalysis: Emulating coumarin biosynthesis with (-)-riboflavin. *J Am Chem Soc* 138:1040–1045.
17. Lechner R, Kümmel S, König B (2010) Visible light flavin photo-oxidation of methylbenzenes, styrenes and phenylacetic acids. *Photochem Photobiol Sci* 9:1367–1377.
18. Megerle U, et al. (2011) Unraveling the flavin-catalyzed photooxidation of benzylic alcohol with transient absorption spectroscopy from sub-pico- to microseconds. *PCCP* 13:8869–8880.
19. Mirzakulova E, et al. (2012) Electrode-assisted catalytic water oxidation by a flavin derivative. *Nat Chem* 4:794–801.
20. Sakai M, Takahashi H (1996) One-electron photoreduction of flavin mononucleotide: Time-resolved resonance Raman and absorption study. *J Mol Struct* 379:9–18.
21. Kao Y-T, et al. (2008) Ultrafast dynamics of flavins in five redox states. *J Am Chem Soc* 130:13132–13139.
22. Warren JJ, Tronic TA, Mayer JM (2010) Thermochemistry of proton-coupled electron transfer reagents and its implications. *Chem Rev* 110:6961–7001.
23. Kowalczyk RM, Schleicher E, Bittl R, Weber S (2004) The photoinduced triplet of flavins and its protonation states. *J Am Chem Soc* 126:11393–11399.
24. Bruice TC (1980) Mechanisms of flavin catalysis. *Acc Chem Res* 13:256–262.
25. Eberlein G, Bruice TC (1982) One and two electron reduction of oxygen by 1,5-dihydroflavins. *J Am Chem Soc* 104:1449–1452.
26. Studer A, Curran DP (2016) Catalysis of radical reactions: A radical chemistry perspective. *Angew Chem Int Ed Engl* 55:58–102.
27. Gentry EC, Knowles RR (2016) Synthetic applications of proton-coupled electron transfer. *Acc Chem Res* 49:1546–1556.
28. Messner KR, Imlay JA (2002) Mechanism of superoxide and hydrogen peroxide formation by fumarate reductase, succinate dehydrogenase, and aspartate oxidase. *J Biol Chem* 277:42563–42571.
29. Klopstra M, Hage R, Kellogg RM, Feringa BL (2003) Non-heme iron catalysts for the benzylic oxidation: A parallel ligand screening approach. *Tet Lett* 44:4581–4584.
30. Masahide Y, Takuya N, Yasumasa K, Tsutomu S (2003) Micelle-enhancing effect on a flavin-photosensitized reaction of benzyl alcohols in aqueous solution. *Bull Chem Soc Jpn* 76:601–605.
31. Churakova E, et al. (2011) Specific photobiocatalytic oxyfunctionalization reactions. *Angew Chem Int Ed Engl* 50:10716–10719.
32. Perez DI, Grau MM, Arends IWCE, Hollmann F (2009) Visible light-driven and chloroperoxidase-catalyzed oxygenation reactions. *Chem Commun (Camb)* (44): 6848–6850.
33. Carroll JB, et al. (2005) Model systems for flavoenzyme activity: Site-isolated redox behavior in flavin-functionalized random polystyrene copolymers. *Org Lett* 7:2551–2554.
34. Tucker JW, Zhang Y, Jamison TF, Stephenson CR (2012) Visible-light photoredox catalysis in flow. *Angew Chem Int Ed Engl* 51:4144–4147.
35. Song N, Dares CJ, Sheridan MV, Meyer TJ (2016) Proton-coupled electron transfer reduction of a quinone by an oxide-bound riboflavin derivative. *J Phys Chem C* 120: 23984–23988.
36. Hanson K, et al. (2012) Photostability of phosphonate-derivatized, Ru(II) polypyridyl complexes on metal oxide surfaces. *ACS Appl Mater Interfaces* 4:1462–1469.
37. Pandiri M, Hossain MS, Foss FW, Rajeshwar K, Paz Y (2016) Enhanced photocatalytic activity of a self-stabilized synthetic flavin anchored on a TiO_2 surface. *Phys Chem Chem Phys* 18:18575–18583.
38. Wee K-R, et al. (2014) Stabilization of ruthenium(II) polypyridyl chromophores on nanoparticle metal-oxide electrodes in water by hydrophobic PMMA overlayers. *J Am Chem Soc* 136:13514–13517.
39. Hanson K, Losego MD, Kalanyan B, Parsons GN, Meyer TJ (2013) Stabilizing small molecules on metal oxide surfaces using atomic layer deposition. *Nano Lett* 13:4802–4809.
40. Dad'ová J, Svobodová E, Sikorski M, König B, Cibulka R (2012) Photooxidation of sulfides to sulfoxides mediated by tetra-o-acetylriboflavin and visible light. *ChemCatChem* 4:620–623.
41. Fukuzumi S, Tanii K, Tanaka T (1989) Flavin-sensitized photo-oxidation of unsaturated fatty acids. *J Chem Soc, Perkin Trans 2* (12):2103–2108.
42. Ogilby PR, Foote CS (1983) Chemistry of singlet oxygen. 42. Effect of solvent, solvent isotopic substitution, and temperature on the lifetime of singlet molecular oxygen (1.Delta.g). *J Am Chem Soc* 105:3423–3430.